

Chapter 3

The CDF Detector

M. Paulini, A.B. Wicklund

3.1 Introduction

The CDF detector has evolved over a twenty year period. CDF was the first experiment at the Tevatron to perform quantitative measurements of b -quark production, using single-lepton and J/ψ samples in Run 0 (1988-1989). CDF was the first hadron collider experiment to successfully employ a silicon vertex detector (SVX). The four layer, axial readout SVX (Run Ia) and SVX' (Run Ib) detectors were used to discover the top quark through detection of the b -quark decay chain. They were also used for a systematic program of b -physics studies, including B -lifetimes, $B\bar{B}$ mixing, discovery of the B_c , and measurement of CP violation in the $B^0 \rightarrow J/\psi K_S^0$ mode. In the course of this program, CDF has developed the techniques to identify B hadron final states in J/ψ and $\ell\nu D$ semileptonic modes, and to flavor tag these states using away-side lepton and jet-charge tags and toward side fragmentation correlations. As a byproduct, CDF has developed control sample strategies to calibrate particle identification using relativistic rise dE/dx , to optimize flavor tagging efficiency, and to measure material effects (energy loss and radiation length corrections) needed for precision mass measurements. CDF has published over fifty papers on B physics with the Run 0 and Run I data. In addition to Run I physics data, CDF recorded data on a variety of specialized triggers in order to estimate rates and backgrounds for the Run II program. Although the Run II B -physics program at CDF will be technically more challenging than Run I, CDF starts with the advantage of extensive experience and benchmark data.

The upgraded CDF detector and physics program for Run II is described in detail in the CDF Technical Design Report [1]. The additional upgrades for time-of-flight and innermost silicon detector are described in the PAC proposal P909 [2]. Below we summarize the Run II detector configuration, with expected performance including particle identification, issues for central solenoidal detectors, CDF B -physics trigger plans, and offline analysis issues.

3.2 CDF Run II Detector

The main upgrades to the CDF detector for Run II can be summarized as follows:

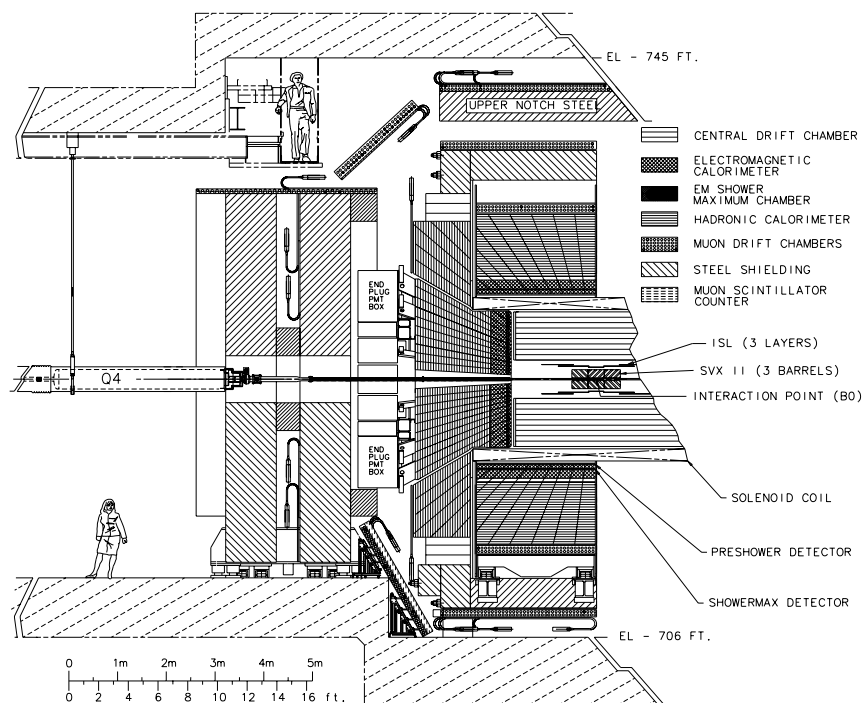


Figure 3.1: Elevation view of the Run II CDF detector

- Fully digital DAQ system designed for 132 ns bunch crossing times
- Vastly upgraded silicon detector
 - 707,000 channels compared with 46,000 in Run I
 - Axial, stereo, and 90° strip readout
 - Full coverage over the luminous region along the beam axis
 - Radial coverage from 1.35 to 28 cm over $|\eta| < 2$
 - Innermost silicon layer (“L00”) on beampipe with 6 μm axial hit resolution
- Outer drift chamber capable of 132 ns maximum drift
 - 30,240 sense wires, 44-132 cm radius, 96 dE/dx samples possible per track
- Fast scintillator-based calorimetry out to $|\eta| \simeq 3$
- Expanded muon coverage out to $\eta \simeq 1.5$
- Improved trigger capabilities
 - Drift chamber tracks with high precision at Level-1
 - Silicon tracks for detached vertex triggers at Level-2
- Expanded particle identification via time-of-flight and dE/dx

COT	
Radial coverage	44 to 132 cm
Number of superlayers	8
Measurements per superlayer	12
Readout coordinates of SLs	$+2^\circ \ 0^\circ \ -2^\circ \ 0^\circ \ +2^\circ \ 0^\circ \ -2^\circ \ 0^\circ$
Maximum drift distance	0.88 cm
Resolution per measurement	180 μm
Rapidity coverage	$ \eta \leq 1.0$
Number of channels	30,240
Layer 00	
Radial coverage	1.35 to 1.65 cm
Resolution per measurement	6 μm (axial)
Number of channels	13,824
SVX II	
Radial coverage	2.4 to 10.7 cm, staggered quadrants
Number of layers	5
Readout coordinates	r- ϕ on one side of all layers
Stereo side	r-z, r-z, r-sas, r-z, r-sas (sas $\equiv \pm 1.2^\circ$ stereo)
Readout pitch	60-65 μm r- ϕ ; 60-150 μm stereo
Resolution per measurement	12 μm (axial)
Total length	96.0 cm
Rapidity coverage	$ \eta \leq 2.0$
Number of channels	423,900
ISL	
Radial coverage	20 to 28 cm
Number of layers	one for $ \eta < 1$; two for $1 < \eta < 2$
Readout coordinates	r- ϕ and r-sas (sas $\equiv \pm 1.2^\circ$ stereo) (all layers)
Readout pitch	110 μm (axial); 146 μm (stereo)
Resolution per measurement	16 μm (axial)
Total length	174 cm
Rapidity coverage	$ \eta \leq 1.9$
Number of channels	268,800

Table 3.1: Design parameters of the CDF tracking systems

$ \eta $ Range	$\Delta\phi$	$\Delta\eta$
0. - 1.1 (1.2 h)	15°	~ 0.1
1.1 (1.2 h) - 1.8	7.5°	~ 0.1
1.8 - 2.1	7.5°	~ 0.16
2.1 - 3.64	15°	0.2 – 0.6

Table 3.2: CDF II Calorimeter Segmentation

The CDF detector features excellent charged particle tracking and good electron and muon identification in the central region. The detector is built around a 3 m diameter 5 m long superconducting solenoid operated at 1.4 T. The overall CDF Run II detector schematic is shown in elevation view in Fig. 3.1. The CDF tracking system includes a central outer drift chamber (COT), a double-sided five layer inner silicon detector (SVX II), a double-sided two layer intermediate silicon tracker (ISL), and a single layer rad-hard detector mounted on the beampipe (L00). COT tracks above 1.5 GeV/c are available for triggering at Level-1 (XFT); SVX layers 0-3 are combined with XFT tracks at Level-2 (SVT). The main parameters of the CDF tracking system are summarized in Table 3.1.

Outside the solenoid, Pb-scintillator electromagnetic (EM) and Fe-scintillator hadronic (HAD) calorimeters cover the range $|\eta| < 3.6$. Both the central ($|\eta| < 1.1$) and plug ($1.1 < |\eta| < 3.6$) electromagnetic calorimeters have fine grained shower profile detectors at electron shower maximum, and preshower pulse height detectors at approximately $1X_o$ depth. Electron identification is accomplished using E/p from the EM calorimeter and also in the shower maximum and preshower detectors; using $HAD/EM \sim 0$; and using shower shape and position matching in the shower max detectors. Together with COT dE/dx , CDF gets $\sim 10^{-3}$ π/e rejection in the central region. The calorimeter cell segmentation is summarized in Table 3.2. A comparison of the central and plug calorimeters is given in Table 3.3.

The calorimeter steel serves as a filter for muon detection in the central (CMU) and extension (CMX) muon proportional chambers, over the range $|\eta| < 1$, $p_T > 1.4$ GeV/c. Additional iron shielding, including the magnet yoke, provides a muon filter for the upgrade muon chambers (CMP) in the range $|\eta| < 0.6$, $p_T > 2.2$ GeV/c. The (non-energized) forward toroids from Run I provide muon filters for intermediate $1.0 < |\eta| < 1.5$ muon chambers (IMU) for $p_T > 2$ GeV/c. Scintillators for triggering are included in CMP, CMX, and IMU. Muon identification is accomplished by matching track segments in the muon chambers with COT/SVX tracks; matching is available in $R\Phi$ for all detectors and in the Z views in CMU and CMX. The muon systems are summarized in Table 3.4.

The Run II CDF detector configuration allows electron and muon identification with drift chamber tracking over the range $|\eta| < 1.0$, with additional coverage out to $|\eta| \sim 1.5$ using stand-alone silicon tracking. Typical thresholds are $p_T > 1$ GeV/c (electrons), $p_T > 1.5$ GeV/c (muons). Calibration of electron and muon identification is accomplished *in situ* with large samples of J/ψ 's and photon conversions.

	Central	Plug
EM:		
Thickness	$19X_0, 1\lambda$	$21X_0, 1\lambda$
Sample (Pb)	$0.6X_0$	$0.8X_0$
Sample (scint.)	5 mm	4.5 mm
WLS	sheet	fiber
Light yield	160 pe/GeV	300 pe/GeV
Sampling res.	$11.6\%/\sqrt{E_T}$	$14\%/\sqrt{E}$
Stoch. res.	$14\%/\sqrt{E_T}$	$16\%/\sqrt{E}$
Shower Max. seg. (cm)	$1.4\phi \times (1.6-2.0)$ Z	0.5×0.5 UV
Pre-shower seg. (cm)	$1.4\phi \times 65$ Z	by tower
Hadron:		
Thickness	4.5λ	7λ
Sample (Fe)	1 to 2 in.	2 in.
Sample (scint.)	10 mm	6 mm
WLS	finger	fiber
Light yield	~ 40 pe/GeV	39 pe/GeV

Table 3.3: Central and Plug Upgraded Calorimeter Comparison

	CMU	CMP	CMX	IMU
Pseudo-rapidity coverage	$ \eta \leq 0.6$	$ \eta \leq 0.6$	$0.6 \leq \eta \leq 1.0$	$1.0 \leq \eta \leq 1.5$
Drift tube cross-section	2.68 x 6.35 cm	2.5 x 15 cm	2.5 x 15 cm	2.5 x 8.4 cm
Drift tube length	226 cm	640 cm	180 cm	363 cm
Max drift time	800 ns	1.4 μ s	1.4 μ s	800 ns
Total drift tubes (present)	2304	864	1536	none
Total drift tubes (Run II)	2304	1076	2208	1728
Scintillation counter thickness		2.5 cm	1.5 cm	2.5 cm
Scintillation counter width		30 cm	30-40 cm	17 cm
Scintillation counter length		320 cm	180 cm	180 cm
Total counters (present)		128	256	none
Total counters (Run II)		269	324	864
Pion interaction lengths	5.5	7.8	6.2	6.2-20
Minimum muon p_T	1.4 GeV/c	2.2 GeV/c	1.4 GeV/c	1.4-2.0 GeV/c
Multiple scattering resolution	12 cm/ p	15 cm/ p	13 cm/ p	13-25 cm/ p

Table 3.4: Design Parameters of the CDF II Muon Detectors. Pion interaction lengths and multiple scattering are computed at a reference angle of $\theta = 90^\circ$ in CMU and CMP, at an angle of $\theta = 55^\circ$ in CMX, and for a range of angles for the IMU.

Photon identification is done using the EM calorimetry, using the preshower and shower maximum detectors to separate π^0/γ . Channels like $B \rightarrow J/\psi\eta$ can be reconstructed with the calorimeter. Rare decays such as $B \rightarrow K^*\gamma$ use photon conversions to obtain precision γ reconstruction.

Asymptotic tracking resolutions are $\sigma(p_T) \simeq 0.0007 p_T^2$ ($|\eta| < 1.1$), and $\sigma(p_T) \simeq 0.004 p_T^2$ ($|\eta| < 2$ -stand-alone SVX tracking). The SVX detectors provide typical impact parameter resolution of 15 ($R - \phi$ - view) and 30 (Z - view) μm . For example, this results in mass resolution of around 20 MeV for $B^0 \rightarrow \pi^+\pi^-$ and proper time resolution of 45 fs for $B_s^0 \rightarrow D_s^-\pi^+$.

Particle identification to separate pions, kaons, protons, and electrons is provided by dE/dx and time-of-flight (TOF) detectors ($|\eta| < 1$):

- $1/\beta^2 dE/dx$ in both COT and SVX
- Relativistic rise dE/dx in COT
 $\simeq 1 \sigma \pi - K$ separation, $p > 2$ GeV/c
- TOF bars outside the COT (1.4 m radius)
 $\simeq 100$ ps resolution

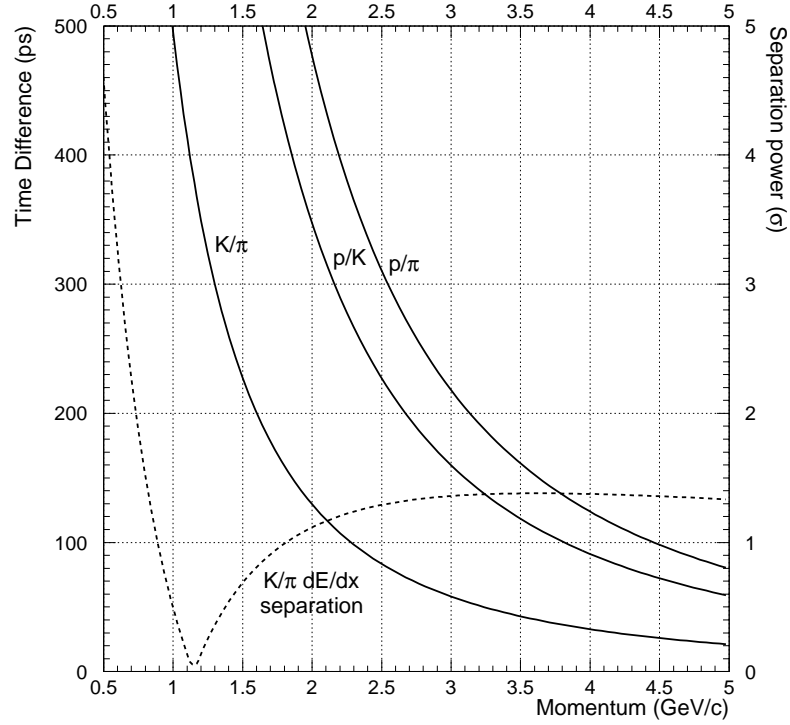


Figure 3.2: Time difference as a function of momentum for π, K, p at a radius of 140 cm, expressed in ps and separation power, assuming 100 ps resolution. The dashed line shows the K/π separation using dE/dx in the COT.

2σ $K - \pi$ separation at 1.5 GeV/c

Figure 3.2 shows the expected separation as a function of momentum. The low momentum particle identification provides flavor tagging with kaons, both on the away side \bar{b} -jet, and on the same side as the trigger B (e.g., B_s^0 correlated with K^+ , \bar{B}_s^0 with K^-); it should also provide useful kaon separation for charm reconstruction, e.g. $B_s^0 \rightarrow D_s^- \pi^+$. Above 2 GeV/c, the COT dE/dx provides a statistical separation of pions and kaons. This will be crucial for determination of CP asymmetries in $B^0 \rightarrow \pi^+ \pi^-$ and $B_s^0 \rightarrow K^+ K^-$. The dE/dx and TOF calibrations can be determined *in situ* using pions and protons from K_S and Λ decays, kaons from $\phi \rightarrow K^+ K^-$, electrons from conversion photons, and muons from J/ψ decay.

3.3 Issues for Central Solenoidal Detectors at the Tevatron

In the Run II detector full charged particle tracking using the SVX and the COT is confined to $\eta < 1.1$. Since all B -physics triggers are track based, and rely on COT tracks in the Level-1 trigger, the B triggers are basically limited to this η range. Furthermore, in order

to achieve a reasonable Lorentz boost for the triggered B hadrons, it is necessary to select events with $p_T(B)$ above some minimum cutoff, typically of order 4-6 GeV/c. In terms of production rates, this is not really a severe limitation. At 10^{32} luminosity, the total $b\bar{b}$ production rate is around 10 kHz at the Tevatron (eg. 10^{11} events per fb^{-1}), much more than the CDF data acquisition rate of $\simeq 75$ Hz to tape. Since B production at high p_T peaks at small $|y|$, the kinematic restriction is such that about 6% of B -hadrons are produced in the region $|y| < 1$ and $p_T > 6$ GeV/c (e.g., 1.2 kHz of $B + \bar{B}$ at 10^{32}).

Thus, the basic trigger strategy is to select B decays to specific final states in the central region, for example $B^0 \rightarrow J/\psi K_S$ or $B_s^0 \rightarrow D_s^- \pi^+$, with charged particle tracks confined to $|\eta| < 1$. For mixing and CP studies, flavor tagging is accomplished using either the away-side \bar{B} or same-side fragmentation correlations. The fragmentation correlations give a highly efficient flavor tag ($\simeq 70\%$ in Run I), since the tagging tracks are guaranteed to be in the central region. The away side tagging would be limited if tracking were confined to $|\eta| < 1$, but the stand-alone SVX tracking extends the coverage in η , and so is expected to greatly improve efficiency for jet-charge and lepton tagging of away-side b -jets.

There are some advantages to the central detector configuration:

- The Tevatron beamspot is small ($\sim 25\mu\text{m}$) in the transverse plane. This feature is exploited at the trigger level in CDF Run II, using the SVX detector to identify large-impact parameter tracks from B decays in the level-2 trigger. This requires the Tevatron beam to be aligned parallel to the detector axis, due to the long ($\sim 60\text{cm}$) luminous region in Z . The SVT- trigger will yield a highly pure sample of inclusive B decays, approximately 10^8 $b\bar{b}$ events per fb^{-1} .
- With the $p_T(B)$ cut, the proper time resolution is adequate for demanding analyses such as B_s mixing (e.g., 45 fs on $B_s \rightarrow D_s^- \pi^+$)
- The $p_T(B)$ requirement also improves the ratio of B production to QCD background. While the total $b\bar{b}$ cross section is of order 0.2% of the minimum bias rate, the high- p_T b -jet cross section is measured to be 2% of the QCD jet rate, in the p_T range of interest for CDF.
- In the central region, tracks are well spread out in Z , and CDF has demonstrated highly efficient track reconstruction for $b\bar{b}$ events.

3.4 Trigger Strategies

The main B -physics goals for CDF Run II make use of the following final states. Of course in each case, other final states, both inclusive and exclusive, are used as calibration samples, and so the triggers must be designed to be inclusive.

- $B^0 \rightarrow J/\psi K_S$ for $\sin 2\beta$
- $B_s^0 \rightarrow J/\psi \phi$ for CP and $\Delta\Gamma$

- $B \rightarrow \mu^+ \mu^- K^{(*)}$ rare decays
- $B_s^0 \rightarrow D_s^- \pi^+$ for B_s mixing
- $B_s \rightarrow D_s^- \ell^+ \nu$ for B_s mixing
- $B_{(s)}^0 \rightarrow K^{*0} \gamma, \phi \gamma$ using photon conversion $\gamma \rightarrow e^+ e^-$
- $B^0 \rightarrow \pi^+ \pi^-$, $B_s^0 \rightarrow K^+ K^-$ for CKM angle γ

This is of course only a partial list. CDF has a three-level trigger design. Level-1 is pipelined so as to be deadtimeless. Digitized data are stored in 42×132 ns buffers to create and count trigger primitives (electrons, muons, COT tracks, and combinations of these). Level-2 is a global trigger that allows finer grained electron and muon track matching, and more sophisticated combinations of trigger primitives (for example, opposite charged lepton pairs with invariant mass requirements). Level-2 finds SVT-tracks using four SVX II layers; these are matched to the XFT/COT tracks found in level-1 to define high resolution, large impact parameter b -decay candidates. Level-2 also matches electrons to the central shower-maximum detector. Finally, Level-3 provides offline quality tracking and calorimeter reconstruction.

Using Run I data, CDF has carefully optimized the use of bandwidth for Run II triggers. The basic trigger requirements can be summarized as follows:

- Dimuons and dielectrons
 - Level-1: Two leptons with COT matched to muon chambers or central calorimeter
 - Level-2,3: Additional mass, charge, and $\Delta\Phi$ cuts
- Single Leptons
 - Level-1: Single leptons matched to muon chambers or central calorimeter
 - Level-2,3: Additional requirement of accompanying SVT track
- B hadronic triggers
 - Level-1: two tracks, opposite charge, $\Delta\Phi$ cuts
 - Level-2,3: two SVX tracks, impact parameter and ct cuts

Thresholds for dilepton and two-track triggers are typically 1.5-2.0 GeV/c, and for single leptons 3-4 GeV/c. Level-3 can make additional cuts in order to divide the data into manageable data sets; for example, a high mass cut will be used to define a $B \rightarrow \pi\pi$ stream based on the two-track triggers, while other SVX track requirements will be used to make a $b \rightarrow c$ generic hadronic sample.

The total trigger bandwidth, including B physics, is designed to be 40 kHz (level-1), 300 Hz (Level-2) and 75 Hz Level-3). Thus, the maximum rate level-3 would be 750 nb at 10^{32} luminosity. B triggers are expected to require about half of that bandwidth. Table 3.5 gives the expected bandwidth requirements for the trigger streams.

Trigger	L1 σ [nb]	L2 σ [nb]	L3 σ [nb]
$B \rightarrow h^+ h^-$	252,000	560	100
$B \rightarrow \mu\mu(X)$	1100	90	40
$J/\psi \rightarrow ee$	18000	100	6
Lepton plus displaced track	9000	130	40

Table 3.5: Trigger rates for the main CDF II B -physics triggers

Physics Channel	Event yield (2 fb^{-1})
$b \rightarrow J/\psi X$	28,000,000
$B^0 \rightarrow J/\psi K_S^0$	28,000
$B_s \rightarrow D_s \pi$	10,000
$B_s \rightarrow D_s \ell \nu$	30,000
$B \rightarrow \mu^+ \mu^- K^{(*)}$	50
$B \rightarrow K^* \gamma$	200
$B \rightarrow \pi\pi, K\pi, KK$	30,000

Table 3.6: Event yields expected from CDF Run II B -physics triggers

3.5 Offline Analysis and Simulation

CDF has estimated rates for literally hundreds of reconstructable decay modes that come in on the lepton or SVT two-track triggers. Table 3.6 lists some examples.

Detailed studies of the physics reach expected for CDF may be found elsewhere in this document. We discuss briefly two issues that enter into calculations of sensitivity, namely flavor tagging and generic simulation.

3.5.1 Flavor Tagging

CDF measured the flavor tagging efficiencies and dilutions for three methods in the Run I mixing and $\sin 2\beta$ analyses: “same side” (fragmentation correlation) tagging, jet-charge tagging, and soft electron and muon tagging. To understand the “same side” tagging at least qualitatively, CDF analyzed B^{**} production using large samples of semileptonic $B \rightarrow D^{(*)} \ell \nu$ decays and applied these to tune the PYTHIA event generator. This gave qualitative agreement with observed same-side tagging efficiencies, including the observed differences between B^0 and B^+ tagging caused by kaons and protons. For jet-charge algorithms, the tagging was optimized initially using PYTHIA and HERWIG event generators, but actual efficiencies and dilutions were measured with data, for example, by fitting the $B^0 \overline{B}^0$ mixing amplitude or by direct comparison of tagging in $B^\pm \rightarrow J/\psi K^\pm$. Soft lepton tags

were calibrated similarly. For the $\sin 2\beta$ analysis the combined tagging efficiency, including correlations between tags, was $\epsilon D^2 = 6.3 \pm 1.7\%$.

CDF extrapolates the Run I efficiencies and dilutions to Run II conditions, taking into account the standalone silicon tracking to $|\eta| \sim 2$, and including kaon tagging based on TOF. This gives estimates of $\epsilon D^2 \sim 9.1\%$ for $B^0 \rightarrow J/\psi K_S$ and $\epsilon D^2 \sim 11.3\%$ for $B_s \rightarrow D_s^- \pi^+$. The basic strategies for calibrating and optimizing the tagging efficiencies for each method would be similar to Run I. For example, the same side tags can be optimized using semileptonic decays $B^{0,+} \rightarrow D^{(*)} \ell \nu$ and $B_s^0 \rightarrow D_s^{(*)} \ell \nu$, including the effects of fragmentation kaons. Opposite side tags can be optimized on the same semileptonic channels, or on inclusive samples such as $b \rightarrow J/\psi X$ (e.g., by comparing tagging rates for prompt and long lived J/ψ 's). Same-side tags for $\sin 2\beta$ can be calibrated using $B^\pm \rightarrow J/\psi K^\pm$ and $B^0 \rightarrow J/\psi K^{*0}$. Opposite side tags would be calibrated using $B^\pm \rightarrow J/\psi K^\pm$. Thus, there are a variety of data channels and cross checks that are available to understand each tagging method. Event generator Monte Carlo's play a role in helping to model same-side tags, including the effects of kaons, and in understanding correlations and variations of dilution with kinematics.

3.5.2 Monte Carlo Issues

CDF has adopted a GEANT based detector simulation for Run II, which is used for optimization of track reconstruction, muon matching, jet energy analysis, SVT response, etc. The calorimeter response has to be tuned to match data from testbeam, Run I, and eventually Run II. It is obviously straightforward to understand the efficiency for signals such as $B^0 \rightarrow \pi^+ \pi^-$, where the generation is trivial, and the detector response depends only on tracking and SVT efficiency. The main concern for B triggers is backgrounds. For lepton-based triggers, these can be estimated from Run I data. For hadronic triggers such as $B^0 \rightarrow \pi^+ \pi^-$, CDF can set limits on backgrounds using Run I data, and can use the PYTHIA generator (plus SVT simulation) to estimate the backgrounds from real $b\bar{b}$ events. The backgrounds that dominate $B^0 \rightarrow \pi^+ \pi^-$ at the trigger level do not appear to come from real $b\bar{b}$ events but from QCD backgrounds that fake the impact parameter trigger; this conclusion comes from comparison of trigger rates with $b\bar{b}$ Monte Carlo, and also by examining Run I data, comparing high mass two-track rates from QCD and real $b\bar{b}$ events. Thus, while CDF can certainly estimate backgrounds from real $b\bar{b}$ events in the SVT two-track trigger sample (these come in due to real b -hadron lifetimes), it cannot reliably simulate "QCD" backgrounds in this sample (these depend critically on offline SVX reconstruction).

References

- [1] The CDFII Collaboration, “The CDF Detector Technical Design Report”, FERMILAB-Pub-96/390-E
- [2] The CDFII Collaboration “Proposal for Enhancement of the CDF II Detector: an Inner Silicon Layer and a Time of Flight Detector”, submitted to the PAC, October 1998